Psychiatry Research: Neuroimaging 265 (2017) 54–64

Contents lists available at ScienceDirect

Psychiatry Research: Neuroimaging

journal homepage: www.elsevier.com/locate/psychresns

Disrupted resting brain graph measures in individuals at high risk for alcoholism

Bharath Holla[a], Rajanikant Panda[b], Ganesan Venkatasubramanian[c], Bharat Biswal[d], Rose Dawn Bharath[b,*], Vivek Benegal[a,**]

[a] Centre for Addiction Medicine, Department of Psychiatry, National Institute of Mental Health and Neurosciences (NIMHANS), Hosur Road, Bangalore, India
[b] Cognitive Neuroscience Centre and Department of Neuroimaging and Interventional Radiology (NIIR), NIMHANS, Hosur Road, Bangalore, India
[c] Translational Psychiatry Laboratory, Department of Psychiatry, NIMHANS, Hosur Road, Bangalore, India
[d] Department of Biomedical Engineering, New Jersey Institute of Technology (NJIT), University Heights, Newark, NJ, USA

ARTICLE INFO

Keywords:
Alcoholism vulnerability
Children of alcoholics (CoAs)
Externalizing behaviors
Graph theory
rsfMRI

ABSTRACT

Familial susceptibility to alcoholism is likely to be linked to the externalizing diathesis seen in high-risk offspring from high-density alcohol use disorder (AUD) families. The present study aimed at comparing resting brain functional connectivity and their association with externalizing symptoms and alcoholism familial density in 40 substance-naive high-risk (HR) male offspring from high-density AUD families and 30 matched healthy low-risk (LR) males without a family history of substance dependence using graph theory-based network analysis. The HR subjects from high-density AUD families compared with LR, showed significantly reduced clustering, small-worldness, and local network efficiency. The frontoparietal, cingulo-opercular, sensorimotor and cerebellar networks exhibited significantly reduced functional segregation. These disruptions exhibited independent incremental value in predicting the externalizing symptoms over and above the demographic variables. The reduction of functional segregation in HR subjects was significant across both the younger and older age groups and was proportional to the family loading of AUDs. Detection and estimation of these developmentally relevant disruptions in small-world architecture at critical brain regions sub-serving cognitive, affective, and sensorimotor processes are vital for understanding the familial risk for early onset alcoholism as well as for understanding the pathophysiological mechanism of externalizing behaviors.

1. Introduction

A family history of alcoholism constitutes a significant risk factor for the development of alcohol use disorders (AUDs) (Cotton, 1979). This risk is further elevated for individuals with a high family loading of early-onset AUD in multiple first- and second-degree relatives (Cloninger et al., 1986; Cotton, 1979; Schuckit, 1985). These individuals at high risk (HR) for AUDs can be reliably differentiated from persons at low risk (LR), even prior to their initiation of alcohol, on a variety of psychological and neurobiological predictors that are not confounded by alcohol (Cservenka, 2016; Hill and O'Brien, 2015). These include excessive externalizing behaviors (Hussong et al., 2008, 2007), atypical brain volumes (Benegal et al., 2007; Hill et al., 2013, 2011, 2009; Venkatasubramanian et al., 2007), atypical task-related functional brain activity (Acheson et al., 2009; Rangaswamy et al., 2004; Schweinsburg et al., 2004; Silveri et al., 2011) and connectivity (Cservenka et al., 2014; Herting et al., 2011; Spadoni et al., 2013; Wetherill et al., 2012). They also differ in neurocognitive measures of executive function (Gierski et al., 2013; Nigg et al., 2004) and attentional processing (Benegal et al., 1995; Hill et al., 1999). These premorbid deficits indicate that the familial susceptibility to alcoholism is likely to be linked to a neurodevelopmental process that may underlie heritable aspects of an AUD.

Externalizing temperaments and disorders (including attention-deficit/hyperactivity disorder (ADHD), oppositional defiant (ODD) and conduct disorders (CD) in childhood and adult ADHD, antisocial personality disorder (ASPD) in young adults) strongly predict vulnerability for early-onset alcohol and other substance use disorders (SUDs) (Brook et al., 2010; Kuperman et al., 2005; McGue et al., 2001). The overlap is so high that SUDs are considered a part of the externalizing-spectrum of disorders (Krueger et al., 2005; Witkiewitz et al., 2013). While family environmental effects do moderate risk vulnerability in offspring outcomes (Jacob et al., 2003; Verhulst et al., 2015), both SUDS and externalizing disorders are estimated to be highly heritable

* Correspondence to: Cognitive Neurosciences Centre, National Institute of Mental Health and Neurosciences, Bangalore 560029, India.
** Correspondence to: Centre for Addiction Medicine, National Institute of Mental Health and Neurosciences, Bangalore 560029, India.
E-mail addresses: hollabharath@gmail.com (B. Holla), drrosedawn@yahoo.com (R.D. Bharath), vbenegal@gmail.com (V. Benegal).

http://dx.doi.org/10.1016/j.pscychresns.2017.05.002
Received 14 September 2016; Received in revised form 3 May 2017; Accepted 4 May 2017
Available online 14 May 2017
0925-4927/

(Bornovalova et al., 2010; Goodwin, 1979; Hicks et al., 2013; Verhulst et al., 2015), and exhibit extensive overlaps in endophenotype measures between them (Salvatore et al., 2015).

Previous studies examining endophenotypic risk for alcoholism and related externalizing disorders, have reported differences in focal brain morphology and activity. However, it is increasingly apparent that these foci represent nodes of aberrant functional brain-networks and a network paradigm is critical for understanding the functional aberrations that are associated with familial-risk for alcoholism (Cservenka et al., 2015a). The resting state functional connectivity has proved to be a useful measure for investigating functionally coupled intrinsic networks in the human brain (Biswal et al., 1995; Fox and Raichle, 2007). Popular methods for analyzing resting-state data include seed-based approaches, independent component analysis, and graph methods (Lee et al., 2013). Graph theory analysis of resting-state fMRI (rsfMRI) data offer powerful tools in characterizing and quantifying the subject specific alterations in the large-scale functional brain network architecture (Bullmore and Sporns, 2009; Rubinov and Sporns, 2010; Sporns et al., 2004).

Graph theory-based approaches model the brain as a complex network represented graphically as a collection of *'N'* nodes denoting neural elements (neurons or brain regions) that are linked by *'E'* edges representing functional connections. Two basic measures that are used to characterize functional brain-networks in graph model are the clustering coefficient (C), which quantifies the local connectivity as an index of network segregation, and the characteristic path length (L), which quantifies the global connectivity as an index of network integration. A typical Erdos-Renyi type of random network is characterized by low local segregation and high global integration, whereas a non-random ordered network has high local segregation with low global integration. A small world network is said to possess best of both worlds, defined by high local segregation as well as high global integration (Watts and Strogatz, 1998), providing an efficient temporospatial system at remarkably low wiring and energy costs (Bullmore and Sporns, 2009). Moreover, such resting state functional brain graph properties exhibit substantial heritability (Fornito et al., 2011; Glahn et al., 2010; Smit et al., 2010, 2008) and have also found applications in characterizing adolescent brain development (Sato et al., 2014; Vogel et al., 2013). As such, these graph measures could be used to decipher distinct neural signatures underlying the developmental vulnerability to externalizing disorders and addictions.

The exact mechanisms underlying familial susceptibility to alcoholism in alcohol-naïve HR offspring are not fully understood, and we primarily hypothesized that the brain regions that are implicated in task-related studies that examine familial vulnerability to alcoholism (Herting et al., 2011; Rangaswamy et al., 2004; Wetherill et al., 2012) may also show disrupted graph-theoretical measures, of segregation and integration, during resting state. Given that the period from early adolescence to young adulthood is a time of heightened risk for the emergence of alcohol abuse, we additionally explored the age-related differences in network segregation measures between the risk-groups, using a cross-sectional approach. We also explored the relationship of externalizing symptom profile and the density of alcoholism family loading with measures of network segregation.

2. Methods

2.1. Participants

The study population consisted of 90 consenting male participants −50 HR alcohol-naïve subjects from high-density AUD families and 40 LR alcohol-naïve control subjects (without a family history of alcohol or other substance dependence, in first degree relatives), matched on age, education, sex, handedness and socioeconomic status. The HR subjects were ascertained by selecting alcohol-naïve male offspring of a treatment-seeking alcohol dependent father from high-density AUD family, recruited from the Centre for Addiction Medicine, National Institute of Mental Health and Neurosciences (NIMHANS), a tertiary care neuropsychiatry hospital in Bangalore, India. A high-density AUD family was identified when the affected father had an established diagnosis of alcohol dependence (DSM-IV criteria) before the age of 25 (early-onset) and had at least two further affected first-degree relatives (parents, siblings and/or other children) with alcohol dependence. All such male offspring (age $\leq$21 years) who fulfilled these criteria were enrolled. The LR subjects were recruited through community advertisement in local schools and hospitals. Subjects were excluded from the assessments if they had any of the following during a detailed clinical interview and physical examination: (1) recent substance use (i.e., positive breath-analyzer test and/or urine screen) or significant lifetime alcohol or substance use (> 1 lifetime alcoholic drinks, > 2 cigarettes/day and/or any other drug use); (2) presence of comorbid psychiatric (exception of sub-syndromal externalizing spectrum), medical, neurological disorder or a history of lifetime or recent use of psychoactive or neurological drugs; (3) presence of contraindications for MRI and (4) lifetime history of head injury, seizures or neurosurgery. Written informed consent and assent were obtained from all participants and their parents in accordance with the NIMHANS Institutional Ethics Review Board.

2.2. Clinical assessments

2.2.1. Assessment of participants

All HR and LR subjects were assessed on the semi-structured assessment for genetics of alcoholism (SSAGA II), child, adolescent or adult versions (Bucholz et al., 1994) as indicated to assess externalizing symptoms specifically and to rule out any other syndromal psychiatric diagnoses. This instrument has previously been translated and used in relevant regional languages (Hindi and Kannada) (Benegal et al., 2007; Venkatasubramanian et al., 2007). The items pertaining to the externalizing spectrum [ADHD, ODD and CD diagnoses from child/adolescent versions (age < 18y); and adult ADHD, ASPD diagnoses from adult version (age 18y+)] were added and proportionally scaled to compute a cross-diagnoses dimensional externalizing symptom score (ESS) (Benegal et al., 2007; Dick et al., 2008; Venkatasubramanian et al., 2007). The symptom counts were square-root transformed to approximate normality and stabilize the variance as per a Box-Cox power transformation analysis (optimal $\lambda = 0.52$) (Snedecor and Cochran, 1989). The Annett's handedness questionnaire (Annett, 1967) was used to ascertain that all subjects were right-handed.

2.2.2. Assessment of parents

The SSAGA II – Adult version was also used to assess alcohol and related disorders as well as in screening out other psychiatric disorders in parents. The Family Interview for Genetic Studies (FIGS) (Maxwell, 1992) was used with three or more adult informants in the family, to document family loading (FL) for alcoholism and to screen for other psychiatric disorders in first-degree relatives. FL was calculated as per family patterns of alcoholism analyses criteria (Turner et al., 1993). Parents and grandparents, with diagnosable AUDs, each contributed a score of 1. Scores for aunts, uncles and siblings were the proportion of AUDs in each of their sibships. The LR subjects had no relatives with a history of AUDs. HR offspring with the mother having diagnosable AUDs or use of alcohol during the index pregnancy were excluded, to rule out fetal alcohol effects. Further, Lewis Murray obstetric complications scale (Lewis and Murray, 1987) was used for recall of the pregnancy history from mother to rule out significant adverse obstetric and perinatal events at birth as a confounding etiology for brain developmental delays or deficits. Socioeconomic status (SES) was ascertained using the revised Kuppuswamy's Socioeconomic Status scale (Kumar et al., 2012). This scale provides a composite three-factor SES index based on education and occupation of the head of the family along with monthly income of the household.

2.3. Image acquisition and data preprocessing

Blood-Oxygen-Level Dependent (BOLD) resting-state functional MRI (rsfMRI) scans covering the whole brain were obtained with a Siemens 3T Skyra MRI (Erlangen Germany) using a 32 channel head coil. The functional data consisted of 153 whole-brain gradient-echo echo-planar images (EPI). The EPI sequence lasted for 5 min and participants were asked to keep their eyes open during the session, lie as quietly as possible, and avoid falling asleep. Both visual confirmation through a video monitor during the scan sequence and a verbal confirmation immediately following the scan sequence controlled for the accuracy of adherence to these instructions. The scan parameters were as follows: repetition time [TR] = 2000 ms; echo time [TE] = 30 ms; flip angle = 78; slice thickness = 3.75 mm; slice order: descending; number of slices = 37; distance factor = 25%; matrix = 64*64*64 mm^3, FOV = 192* 192 mm^2, voxel size = 3*3*3.75 mm^3. After obtaining the fMRI images, a T1-weighted, three-dimensional, high-resolution imaging was performed for anatomical co-registration and segmentation. The T1-Magnetization-Prepared Rapid Acquisition with Gradient Echo (MPRAGE) was acquired with TR = 1900 ms, TE = 2.43, TI = 900 ms, FOV = 240*240 mm^2 yielding 192 sagittal slices and a voxel size of 1*1*1 mm^3.

The functional and structural MRI preprocessing were performed using SPM8 (SPM8; Wellcome Department of Cognitive Neurology, London) (http://www.fil.ion.ucl.ac.uk/spm/). The first three functional images were discarded to allow for signal equilibration and to provide time for habituation of the subject in the scanner. Preprocessing steps included: realignment, slice-time correction, co-registration followed by segmentation of the structural data for regressing out the white matter and CSF effects and normalization to MNI152 standard space of 3x3x3mm^3. The two groups did not differ in the amount of warping required to fit the images to MNI space [$t = 0.54$, $p = 0.60$, HR = 26.6 ± 5.9%, LR = 25.8 ± 6.15%]. Because rsfMRI is sensitive to micro head movements, following additional preprocessing steps were applied to reduce motion artifacts. First, subjects with a maximum head movement of > 1.5 mm (half a voxel's width) in any axis were excluded [n = 16 (HR = 7, LR = 9)]. Second, a frame-wise displacement (FD) scalar was computed for each participant ($FD_i = |\Delta d_{ix}| + |\Delta d_{iy}| + |\Delta d_{iz}| + |\Delta \alpha_i| + |\Delta \beta_i| + |\Delta \gamma_i|$), where $\Delta d_{ix} = d_{(i-1)x} - d_{ix}$, and similarly for the other five rigid body parameters [dix diy diz αi βi γi]) to estimate the volume-by-volume micro-movements in the six rigid body parameters (Power et al., 2012, 2015). Subjects with mean FD > 0.25 mm were also excluded [n = 4 (HR = 3, LR = 1)]. Thus, after excluding these 20 subjects (10 in each of HR and LR group), the final sample comprised of 70 subjects (HR = 40, LR = 30). The excluded subjects did not differ in clinical or demographic variables when compared to the final sample (HR: age: t = −0.6, p = 0.5; education: t = −0.7, p = 0.4; SES: t = −0.9, p = 0.3; FL: t = 1.3, p = 0.2; ESS: t = −0.5, p = 0.6; LR: age: t = 0.5, p = 0.6; education: t = 0.6, p = 0.4; SES: t = −0.1, p = 0.9; ESS: t = 1.1, p = 0.3). For the remaining 70 subjects, motion correction was further carried out using Friston 24-parameter model regression (3 translations, 3 rotations, 3 translations and 3 rotations shifted 1 volume before, and the 12 corresponding quadratic terms to control for non-linear influences) on the unsmoothed normalized data (Friston et al., 1996). Also, the data was temporally band-pass filtered (0.01–0.09 Hz) to minimize the effects of low frequency drift and high frequency noise.

2.4. Brain network construction

The Dosenbach's 160 ROI (Dos-160) template was used to parcellate the brain into functionally segregated ROIs that covered most of the cortex (Supplement Table S1). The ROIs in this template were derived based on prior meta-analytic studies of cognitive control, error processing, default mode, memory, language and sensorimotor functions (Dosenbach et al., 2010). The nodes of functional networks were extracted from rsfMRI data into 160 spheres (radius = 5 mm) of the Dos-160 template using MarsBaR toolbox® (http://marsbar.sourceforge.net). The time series of an ROI was the average of all the voxels in that ROI. The rsfMRI time series were correlated region by region for each subject across the length of the time series (L = 150), and a 160*160 matrix was constructed for each subject by applying a correlation threshold T (Fisher's r-to-z) to the Pearson's correlation coefficients using a sparsity-based method. Popular techniques to threshold brain network matrix include, sparsity-based and weight-based methods. A weight based technique, often results in network matrices with unequal connection density. This can be problematic because graph-theoretical measures can vary as a function of the number of edges in the network. Sparsity-based thresholding explicitly addresses this problem. With this method, T is allowed to vary across subjects to achieve a desired, fixed connection density.

2.5. Graph theory analysis

The graph metrics of the functional brain-networks were defined on the basis of a 160*160 graph, G(N, E), where G is a non-zero subset with nodes (N = ROIs) and edges (E = intermodal correlation coefficients, Fisher's Z values) as a measure of functional connectivity between nodes calculated using the Brain Connectivity Toolbox (http://www.brain-connectivity-toolbox.net/). To characterize the graph properties of the functional brain-networks, following network metrics were computed using MATLAB® scripts developed in-house. The global metrics comprised: (1) small-world parameters including clustering coefficient (C_p), characteristic path length (L_p), normalized clustering coefficient (γ), normalized characteristic path length (λ) and small-worldness (σ); and (2) network efficiency including global efficiency (E_{Glob}) and local efficiency (E_{Loc}). The regional metrics consisted of nodal normalized clustering coefficient (C_i) and efficiency (e_i). The definitions and the descriptions of the various network parameter measured in the current study are summarized in Table 1 (Rubinov and Sporns, 2010).

To enable comparison of global network properties across groups and participants, we used sparsity threshold to ensure the same number of network edges for each participant by retaining only those connections whose edge strengths exceed a given threshold. To avoid biases associated with using a single threshold, we determined a range of sparsity according to the following criteria (Fornito et al., 2010; Watts and Strogatz, 1998): (1) the average degree of all nodes of each network was larger than 2*log (N). N is the number of nodes (here, N = 160); (2) The γ scalar of each threshold network was larger than 1.1 for all subjects. By this procedure, the range of sparsity ($0.06 \leq S \leq 0.45$, with an increment of $\Delta S = 0.01$) was generated. This procedure guaranteed that the thresholded networks were estimable for small-worldness and also avoids excess network fragmentation at sparser thresholds (Fornito et al., 2010).

2.6. Statistical analysis

The socio-demographic, behavioral and clinical data were tested for normality using the Shapiro-Wilk test and appropriate statistics were used. Statistical comparisons of the global graph metrics, between the two risk groups, were done at both individual sparsity threshold and by using an integrated network summary scalar. The integrated measure provides a summary score over the entire sparsity range, making it more sensitive at identifying brain network graph metric alterations than a single sparsity threshold method (Achard and Bullmore, 2007; He et al., 2009). For a given scalar, the integrated global metric was defined as

$$X_{glob}^{int} = \sum_{k=6}^{45} X(k\Delta S)\Delta S,$$

where ΔS is the sparsity interval of 0.01, and $X(k\Delta S)$ is one of the global

Table 1
Mathematical definitions and description of the various network parameters of the graph $G(N, E)$ with N nodes and E edges measured in the current study.

Network parameters	Description	Definition
Nodal clustering coefficient (C_i)	It reflects the degree of local interconnectivity or segregation among the neighbors of a given node. The C_i of a node is the ratio between the number of existing connections (E) and the number of all possible connections between the nodes in the neighborhood.	$C_i = \frac{2E_i}{k_i(k_i-1)}$
Clustering coefficient (C_p^{Abs})	It is the average of the clustering coefficients over all nodes in the network. It quantifies the local interconnectivity of a network and the degree to which regions cluster or segregate.	$C_p^{Abs} = \frac{1}{n}\sum_{i\in N} C_i$
Characteristic path length (L_p^{Abs})	It is the shortest path length required to link two nodes (i, j), averaged over all pairs of nodes. It is measured as the mean harmonic distance between all possible pairs of nodes and indicates the level of network integration.	$L_p^{Abs} = \frac{1}{n}\sum_{i\in G}\frac{1}{N-1}\sum_{i\neq j\in N}\min\{L_{i,j}\}$
Normalized clustering coefficient (γ)	It is the ratio of the absolute clustering coefficient to averaged clustering coefficient of 1000 matched random networks that keep the same number of nodes, edges, and degree distributions as the real networks for each sparsity level to obtain a difference distribution. A high γ is characterized by densely connected local clusters indicates a higher level of global network segregation.	$\gamma = \frac{C_p^{Abs}}{C_p^{Rand}}$
Normalized characteristic path length (λ)	It is the ratio of the absolute characteristic path length to the averaged characteristic path length of 1000 matched random networks that keep the same number of nodes, edges, and degree distributions. A network with a low λ is characterized by short distances between any two nodes and indicates a higher level of global network integration.	$\lambda = \frac{L_p^{Abs}}{L_p^{Rand}}$
Small Worldness (σ)	It is the ratio between network segregation (γ) and network integration (λ). Small world networks are characterized by high normalized clustering coefficient ($\gamma > 1$) and low normalized characteristic path length ($\lambda \approx 1$) compared to random networks, such that, $\sigma > 1$.	$\sigma = \frac{\gamma}{\lambda}$
Global efficiency (E_{Glob})	It is the average of the inverse of the shortest path lengths in a network and indicates the global efficiency of parallel information transfer in the network.	$E_{Glob}(G) = \frac{1}{N(N-1)}\sum_{i\neq j\in G}\frac{1}{d_{ij}}$
Local efficiency (E_{Loc})	It is the inverse of the average shortest path connecting the given node with all other nodes and indicates the efficiency of a given node in communicating with the rest of the brain.	$E_{Loc}(G) = \frac{1}{N}\sum_{i\in G} E_{Glob}(G_i)$

network metric (γ, λ, σ, E_{Glob} and E_{Loc}) at a sparsity of kΔS. Similarly, the integrated nodal metric for a node i was defined as

$$Y_{nod}^{int}(i) = \sum_{k=6}^{45} Y(i, k\Delta S)\Delta S,$$

where *Y(i,kΔS)* represents the nodal parameter (C_i, e_i) of the node *i* at a sparsity of kΔS. Multiple comparisons correction was carried out for the global and regional network measures using the False Discovery Rate (FDR) set at 5% calculated using the Benjamini-Hochberg procedure (http://go.warwick.ac.uk/tenichols/software/fdr/FDR.m). Further, the brain regions showing significant differences in the two groups were identified and rendered on a brain surface model using the BrainNet Viewer (http://www.nitrc.org/projects/bnv/).

2.7. Relationship between graph-theoretical measures and clinical parameters

To explore relationship between altered network measures and clinical parameters, we used Pearson's correlation analysis. Also, a hierarchical regression analysis was performed to evaluate if the network alterations had unique incremental explanatory power in predicting ESS over and above the demographic variables. Standardized residuals and Cook's distance were examined to ensure that there are no outliers and influential cases. Multicollinearity between predictor variables was checked using a threshold for variance inflation factor (VIF) set at < 1.5. To explore the influence of age, the entire sample was subdivided into four groups (age ≤14 and > 14 years, the median age of the entire sample was 14 years), namely younger HR (n = 23), younger LR (n = 14), older HR (n = 17) and older LR (n = 16). To examine the effect of AUD family loading (FL), the entire group was further subdivided into three groups, FL = 0 (n = 30, all LR), FL < 2.3 (FL score < 2.3 and ≠0, n = 19) and FL > 2.3 (FL score > 2.3, n = 21) (the median FL score in HR group was 2.32). A one-way ANOVA was conducted among the age and FL sub-groups to examine their specific influence on nodal clustering (C_i) values. Additionally, we also examined the regression slopes of C_i for age within both groups and for FL within HR group. Because these analyses were exploratory in nature, we used a statistical significance level of $P < 0.05$ (uncorrected).

3. Results

3.1. Demographic comparisons

Seventy subjects were included in the final graph theory analyses of resting state functional connectivity (40 h, 30LR). The clinical and demographic characteristics of the samples are described in Table 2. They were all right-handed, alcohol naïve, adolescent and young adults. The groups did not differ in mean age (HR = 14.3 ± 3.7 years, LR = 14.9 ± 3.9 years), total gray matter volume, years of education, and socioeconomic status. The HR group had a high FL of alcoholism and significantly greater total externalizing scores. The head motion parameters during the rsfMRI scan did not differ between the two groups and showed no significant correlation with clinical parameters or network metrics (ESS: $r = 0.01$, $p = 0.93$; FL: $r = -0.01$, $p = 0.92$; γ: $r = -0.07$, $p = 0.57$; λ: $r = 0.08$, $p = 0.49$; σ: $r = -0.08$, $p = 0.5$; E_{Loc}: $r = -0.02$, $p = 0.84$; E_{Glob}: $r = -0.01$, $p = 0.95$).

Table 2
Clinical and demographic profile.

	HR[a] (Mean ± SD) (n = 40)	LR[b] (Mean ± SD) (n = 30)	P value (2-tailed)
Age (years)[c]	14.25 ± 3.71	14.90 ± 3.98	0.49
Education (years)	8.57 ± 2.92	8.70 ± 3.49	0.87
Socioeconomic status[d]	11.22 ± 3.30	11.57 ± 1.99	0.59
Head displacement (mm)			
Maximum	0.55 ± 0.34	0.56 ± 0.28	0.85
Framewise	0.14 ± 0.04	0.13 ± 0.04	0.32
Total gray matter volume (ml)	732.38 ± 62.74	719.75 ± 50.33	0.39
Externalizing symptom score[e]	3.86 ± 0.59	1.89 ± 0.73	< 0.001
AUD family loading[f]	2.26 ± 0.51	0	–

[a] High Risk offsprings from multiplex AUD families.
[b] Low Risk healthy controls from community families.
[c] Age range was 8–21 years in both HR and LR groups.
[d] Three-factor socioeconomic index of Kuppuswamy for Indian urban families, revised 2012.
[e] Square-root transformed summative counts of externalizing symptoms.
[f] Family loading of Alcohol Use Disorders (AUD) calculated as per Turner et al. (1993).

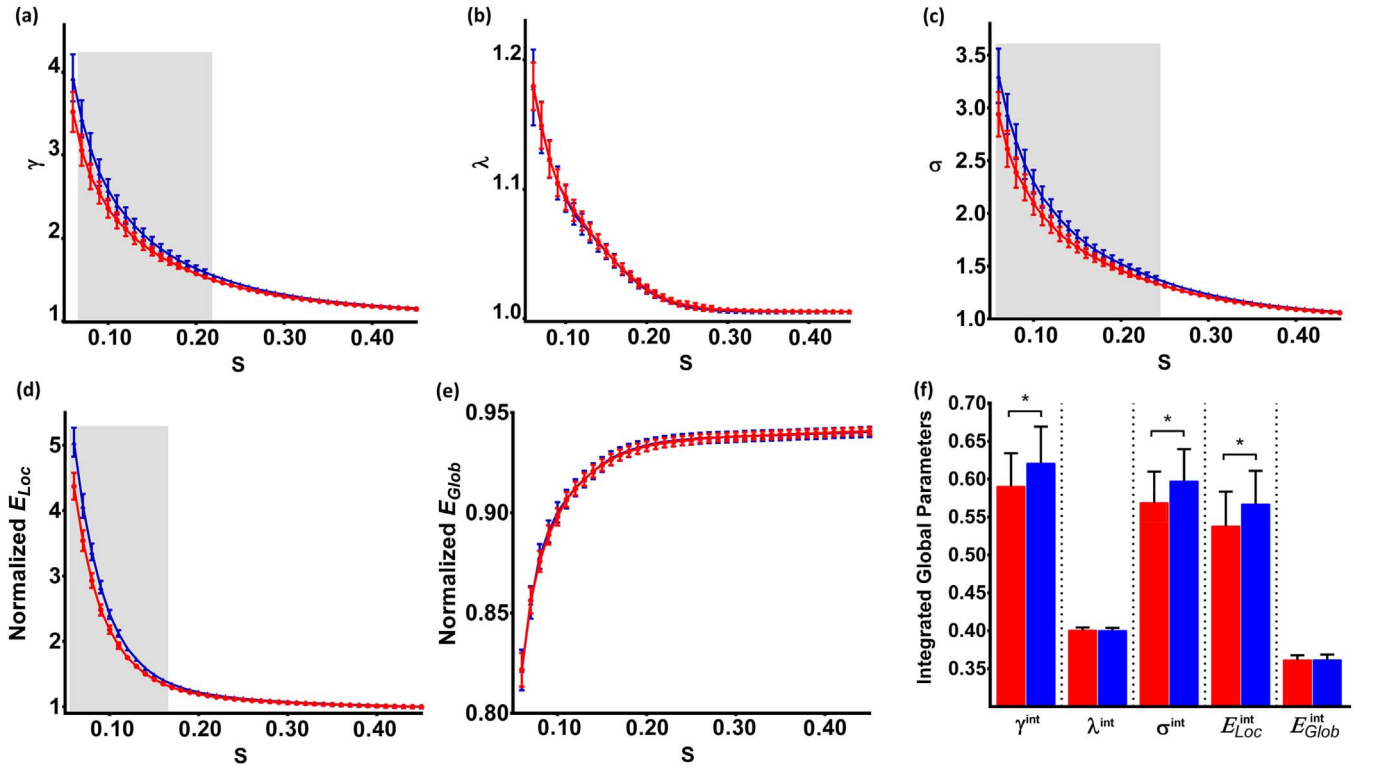

Fig. 1. Graphical representation of the whole-brain small-world network results in high-risk (HR) and low-risk (LR) groups. The graphs (a-e) show comparison of mean and standard errors for (a) Normalized clustering coefficient (γ); (b) Normalized Characteristic Path length (λ); (c) Small-worldness (σ); (d) Normalized Local Efficiency (E_{Loc}); (e) Normalized Global Efficiency (E_{Glob}) between the HR (Red line) and LR (Blue line) groups over the network sparsity threshold S ($0.06 \leq S \leq 0.45$, with increment of 0.01). Shaded areas indicate the range of sparsity thresholds where between-group differences were statistically significant ($p < 0.05$, FDR). (f) The bar plots demonstrate between-group differences in the integrated global parameters. The symbol (*) indicates significant reduction in HR (Red) group compared to LR (Blue) group ($p = 0.006$, $p = 0.004$, $p = 0.004$ for γ, σ and E_{Loc} respectively). (For interpretation of the references to color in this figure legend, the reader is referred to the web version of this article.)

3.2. Differences in global network parameters

The whole-brain functional networks for both groups showed typical features of small-world properties ($\gamma > 1$ and $\lambda \approx 1$). However, compared with matched LR controls, the HR offspring exhibited significantly reduced normalized clustering coefficient (γ), small-worldness (σ) and normalized local efficiency with comparable normalized characteristic path length (λ) and normalized global efficiency over a wide range of sparsity thresholds (γ: $0.07 \leq S \leq 0.21$; σ: $0.06 \leq S \leq 0.24$; E_{Loc}: $0.06 \leq S \leq 0.16$). To address the potential confounds including age, education, SES, head motion and total gray matter volumes, the statistical comparisons of the integrated global parameters were done after regressing out these confounds. Having accounted for their influence, we still found a significant reduction in γ, σ and E_{Loc} [γ: $F(1,63) = 7.98$, $p = 0.006$, $\eta^2 = 0.112$; σ: $F(1,63) = 8.74$, $p = 0.004$, $\eta^2 = 0.122$; E_{Loc}: $F(1,63) = 9.17$, $p = 0.004$, $\eta^2 = 0.127$] (See Fig. 1: a–f).

3.3. Differences in regional nodal parameters

The brain regions that demonstrated significant decreases in the normalized nodal clustering coefficient (C_i^{int}) in HR offspring were lateralized to right cerebral (sub-regions of frontoparietal, cingulo-opercular, sensorimotor networks) and left cerebellar hemispheres (See Table 3 and Fig. 2). There were no region which showed increased C_i^{int} values in HR group. For the nodal efficiency (e_i^{int})measures, there were no significant between group differences that survived multiple comparisons correction.

3.4. Relationship between small-world connectivity differences and clinical parameters

Bivariate correlations revealed a significant negative correlation of the ESS with the normalized nodal clustering coefficient values at right dlPFC ($r = -0.469$, $p < 0.001$), right IPL ($r = -0.375$, $p = 0.001$), right dACC ($r = -0.373$, $p = 0.001$), right parietal sensorimotor cortex ($r = -0.379$, $p = 0.001$), and left inferior cerebellum ($r = -0.398$, $p = 0.001$) indicating that reduced functional segregation in these brain regions was associated with greater severity of externalizing symptoms across the groups (Fig. 3A-E). As ESS had a significant negative correlation with age ($r = -0.350$, $p = 0.003$), a hierarchical regression analysis was performed to evaluate if each of the network alterations had unique incremental explanatory power in predicting the ESS over and above the demographic variables. The order of entry of predictor variables and the results of the five models are presented in Table 4. The first model (demographic variables) was significant $F(2, 67) = 4.82$, $p = 0.011$, $R^2 = 0.126$. Further, the second (frontoparietal), third (cingulo-opercular) and fifth (cerebellar) models exhibited significant independent incremental value in the overall predictability of the model over and above the demographic variables, $F(4,65) = 9.02$, $p = < 0.001$; $F(5,64) = 9.58$, $p = < 0.001$ and $F(7,62) = 8.44$, $p = < 0.001$ respectively. The final model significantly accounted for 48.8% (Model 1 = 12.6%; Models 2–5 = 36.2%) variance in the ESS. The standardized β-coefficient of all the predictors indicated a negative effect on ESS.

To examine the effects of age, a general linear model (ANCOVA) with age, group, and age × group as regressors of the nodal clustering coefficient value (C_i^{Avg}) was examined. Because of the exploratory nature of these analyses, we used the average nodal clustering coefficient of the significant nodes as the dependent variable instead of fitting a linear model on each node separately. For C_i^{Avg}, age × group interaction was significant $F(1,66) = 6.32$, $p = 0.014$, suggesting significantly different regression slopes of age between the groups. To illustrate this interaction, $C_i^{Avg}$was regressed on age within each group and slopes were tested to determine if they differed from zero. The LR

Table 3
Brain regions that showed significant decrease in the normalized clustering coefficient in HR when compared to LR.

Brain regions	Hemisphere	MNI co-ordinates			T	P*
		X	Y	Z		
Fronto-parietal network						
Dorsolateral Pre-Frontal Cortex (dlPFC)	R	46	28	31	−4.55	< 0.0001
Inferior Parietal Lobule (IPL)	R	44	−52	47	−3.70	0.00069
Cingulo-opercular network						
Dorsal Anterior Cingulate (dACC)	R	9	20	34	−3.60	0.00068
Sensorimotor network						
Parietal Gyrus	R	18	−27	62	−3.88	0.00021
Cerebellar network						
Inferior Cerebellum	L	−34	−67	−29	−3.69	0.00035

* *P*-value corrected for multiple comparisons with false discovery rate < 0.05.

subjects in fact exhibited a significantly positive relationship $F(1,28) = 9.71$, $p = 0.004$, $R^2 = 0.257$, with nodal clustering increasing with age. In contrast, for the HR subjects the regression slope did not differ from zero $F(1,38) = 0.10$, $p = 0.75$, $R^2 = 0.003$, remaining approximately the same with age (Fig. 4A). To illustrate the main effect of age on C_i^{Avg}, we subdivided the HR and LR groups using median split (median age = 14y) and conducted a one-way between-group ANOVA among the four groups. This yielded a statistically significant effect $F(3,66) = 19.02$, $p < 0.001$, $\eta^2 = 0.464$. Further, a post-hoc Tukey test revealed that the HR offspring had significantly reduced clustering in both the younger (M1 = 1.25 ± 0.08, M2 = 1.40 ± 0.11, $p < 0.001$) and older (M1 = 1.26 ± 0.09, M2 = 1.43 ± 0.09, $p < 0.001$) groups. Interestingly, younger subjects in the LR group had significantly better clustering than even subjects in the older HR group ($p < 0.001$) (Fig. 4B).

The regression of C_i^{Avg}on FL score within HR group revealed a significant negative relationship $F(1,38) = 8.83$, $p = 0.005$, $R^2 = 0.189$, with nodal clustering reducing with greater FL score (Fig. 4C). To further illustrate the graded risk across the HR and LR groups, we subdivided the HR group using median split (median FL = 2.3) and conducted a one-way between-group ANOVA among the three groups. This yeilded a significant effect $F(2,67) = 33.38$, $p < 0.001$, $\eta^2 = 0.499$. A post-hoc Tukey test revealed significantly reduced clustering in HR groups [FL < 2.3 (1.29 ± 0.08, $p < 0.001$) and FL > 2.3 (1.22 ± 0.06, $p < 0.001$)] compared to the LR group (FL = 0) (1.42 ± 0.09) group. Also, the FL > 2.3 group had significantly reduced clustering compared to the FL < 2.3 group ($p = 0.016$) (Fig. 4D).

4. Discussion

The current study utilized a novel application of graph theory analysis of resting state functional networks to assess the familial risk for alcoholism and mapped them with the phenotypic manifestation of externalizing behaviors. Our results suggest that the functional brain-networks of HR offspring are characterized by disrupted graph-theoretical properties at both the global and regional levels. Moreover, as these abnormalities in the resting state functional network architecture predate any significant alcohol use, they represent premorbid familial vulnerability for alcoholism and are not confounded by alcohol-induced neurotoxicity.

4.1. Small-world characteristics of HR offspring

The human brain is a complex network with various important topological attributes including small-worldness, and high efficiency at low wiring cost (Bullmore and Sporns, 2009; Sporns et al., 2004). The HR offspring from high-density alcoholism families, in this study, exhibited significantly reduced clustering, small-worldness and local efficiency but comparable path lengths and global efficiency relative to matched LR individuals with no family history of alcohol or drug dependence. The reduction in clustering assumed significance in frontoparietal, cingulo-opercular, sensorimotor and cerebellar networks.

The aberrant resting brain graph properties observed in HR offspring indicate a disruption of the balance between the measures of functional segregation and integration in the energy-efficient organization of the human functional brain-networks. Specifically, the reduction in clustering co-efficient values (functional segregation) in HR offspring suggest a limited ability of their brain-networks, to segregate information flow for specialized processing regionally and also within the whole-brain network. Further, as the characteristic path length values (functional integration among multiple, spatially distributed brain regions) was comparable between the groups, the reduction in the small worldness was predominantly due to the reduction of local segregation in HR subjects. Also, the HR subjects demonstrated reduced local network efficiency despite preserved global efficiency. Consistent with studies that have used large scale network analysis of white matter tracts in typically developing subjects (Chen et al., 2013), these functional differences could be reflective of underlying dynamic differences in trajectories of cortical gray and white matter maturation. This pattern of disruption in the network architecture of the HR offspring, with impaired functional segregation (clustering) but spared functional integration (path lengths), represents a shift away from the optimum small-world network organization.

4.2. Disrupted small-world characteristics in manifestation of externalizing behaviors

Externalizing behaviors are considered strong risk factors for early-onset problem alcohol use (Kuperman et al., 2005; McGue et al., 2001). Consistent with substantial previous literature (Benegal et al., 2007; Hussong et al., 2008, 2007; Venkatasubramanian et al., 2007), the HR offspring in the present study had significantly higher scores of externalizing symptoms than the LR group. Importantly, there was a strong inverse correlation between the regional clustering coefficient values across various networks and the expressed externalizing behaviors of the subjects. Together with age, these network abnormalities incrementally predicted around 49% variance in scores of externalizing symptoms. Several brain regions, including right dlPFC-IPL, right dACC, right sensory parietal cortex and left inferior cerebellum, demonstrated reduced clustering coefficient values indicating reduced ability to segregate and specialize information flow efficiently in these regions. Functional abnormalities in these brain regions have previously been reported in seed based functional connectivity studies examining familial risk for alcoholism (Herting et al., 2011; Spadoni et al., 2013; Wetherill et al., 2012) as well as in graph theory based studies of externalizing disorders like ADHD (Cortese et al., 2012; Fair et al., 2012; Sripada et al., 2014).

The brain regions, implicated here, have high functional relevance to the externalizing diatheses and the vulnerability to addictions seen in HR children. Specifically, the abnormalities in frontoparietal and

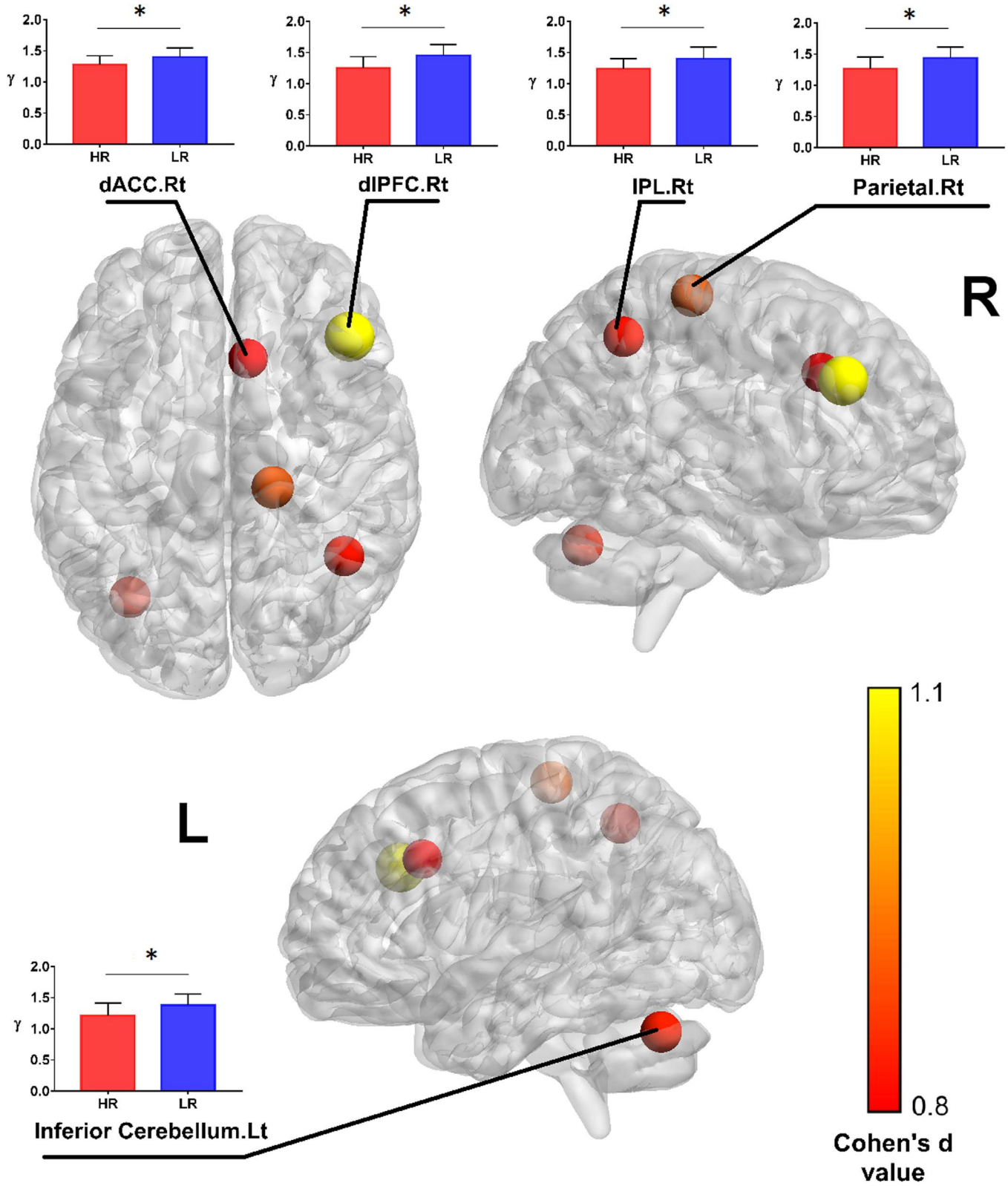

Fig. 2. Surface visualization of the brain regions showing significant reductions in the integrated nodal clustering coefficient values (γ) in high-risk (HR) offspring when compared to low-risk (LR) group. The bar plots demonstrate the γ values for the two groups at different brain regions and the symbol (*) indicates significant reduction (p-value < 0.05, FDR corrected). Nodal size is proportional to the T-value and the color map is indicative of the Cohen's d value. All regions had Cohen's d value > 0.8 indicating large effect sizes. (For interpretation of the references to color in this figure legend, the reader is referred to the web version of this article.)

cingulo-opercular networks, which represent a dual-system for top-down executive control, are critical (Dosenbach et al., 2007). The dorsal anterior cingulate cortex and cingulo-opercular system provide stable control (set-maintenance) during task-performance (Dosenbach et al., 2006), by continuously monitoring for errors. On the other hand, the dorsolateral prefrontal cortex, and the frontoparietal system are triggered by error cues and exert adaptive control by rapidly resolving such errors (MacDonald et al., 2000). Defects in these dual-mechanisms

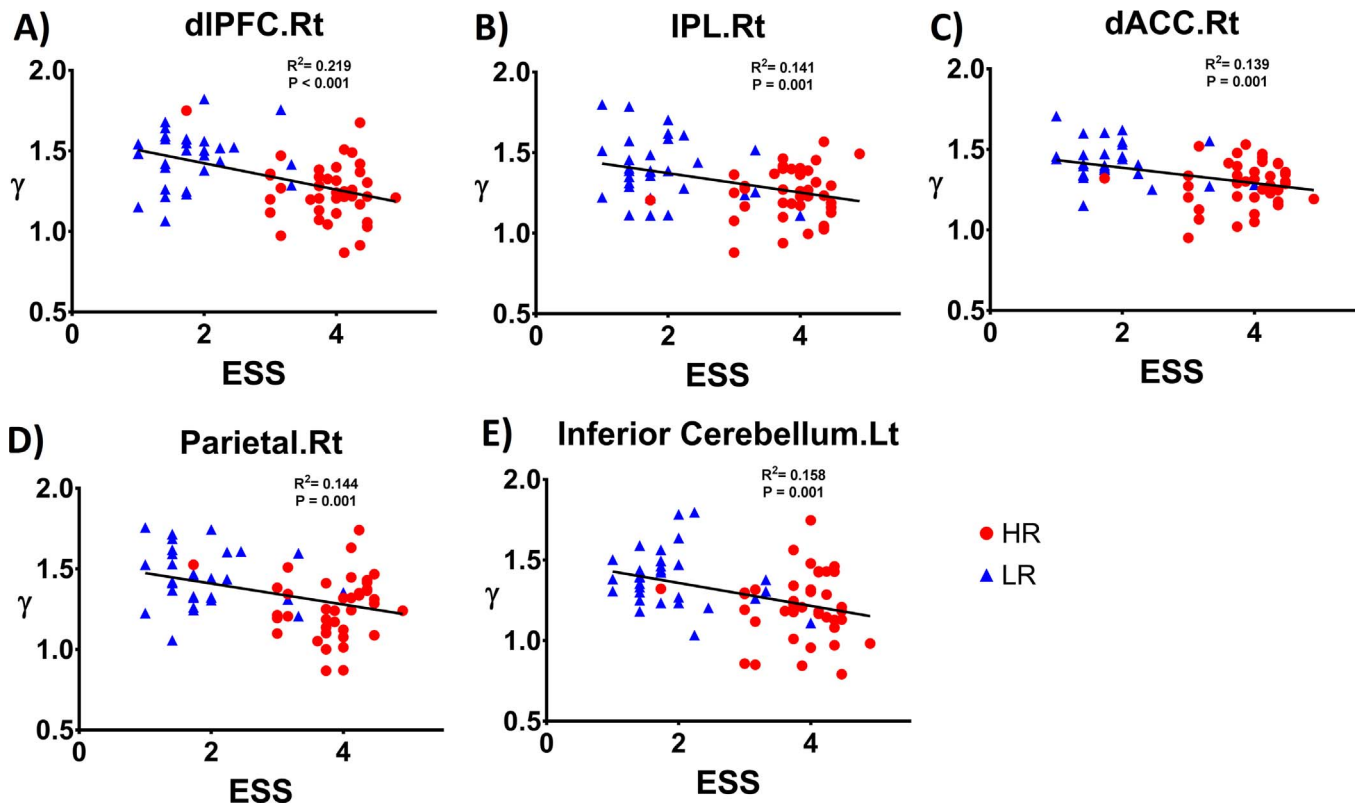

Fig. 3. Scatter plots of the normalized nodal clustering coefficient values (γ) in high-risk (HR) and low-risk (LR) groups changing with the externalizing symptom score (ESS) (square-root transformed) at (A) dorsolateral Pre-Frontal Cortex (dlPFC), (B) Inferior Parietal Lobule (IPL), (C) dorsal Anterior Cingulate (dACC), (D) parietal gyrus, and (E) left inferior cerebellum. Subjects with greater externalizing symptoms exhibited significantly reduced clustering co-efficient values, a measure of functional segregation.

Table 4
Hierarchical Regression Models Predicting Externalizing Symptom Score across the groups (n = 70).

Predictor variable	Externalizing Symptom Score[a]				
	R^2	ΔR^2	p-value (F change)	Beta	p-value (Beta)
Step 1: Demographic variables	0.126	0.126	**0.011**		
Age				−0.295	**0.004**
SES				−0.056	0.549
Step 2: Fronto-Parietal Network	0.357	0.231	< **0.001**		
dlPFC				−0.282	**0.017**
IPL				−0.071	0.521
Step 3: Cingulo-Opercular Network	0.428	0.071	**0.006**		
dACC				−0.214	**0.031**
Step 4: Sensorimotor network	0.453	0.024	0.099		
Parietal Gyrus				−0.152	0.127
Step 5: Cerebellar network	0.488	0.035	**0.042**		
Inferior Cerebellum				−0.206	**0.042**

[a] Square-root transformed summative counts of externalizing symptoms. dlPFC, Dorsolateral Pre-Frontal Cortex; IPL, Inferior Parietal Lobule; dACC, Dorsal Anterior Cingulate; Significant results are highlighted in bold text; Beta indicates standardized regression coefficients with all the predictors entered.

that provide stability and adaptability, may ultimately result in an apparent failure to recognize and learn from mistakes (Hauser et al., 2014). Additionally, the cerebellar network implicated in this study, is known to interact with this dual-system in mediating the top-down control (Dosenbach et al., 2008). Our findings suggest that even prior to developing alcohol dependence or addiction, youth with familial history of alcoholism already exhibit deficits in functional networks relevant for top-down executive control that is similar to those seen in AUD adults (Beck et al., 2012). Although these network alterations could be a function of both heritable and family environmental factors that exist in high-density AUD families, it could explain the heightened risk of formation of drug habit in HR offspring and the subsequent inability to break an established drug habit (Bechara et al., 2002).

4.3. Small-world characteristics within age and AUD family-loading groups

Our results indicate significant and robust differences in functional network segregation measures for both the younger and older age groups, presumably reflecting aberrant maturation of the functional network architecture in the HR offsprings. Additionally, the younger LR group already exhibited significantly better clustering than the older HR group, indicating severe developmental differences in the ability of the affected brain regions for segregated neural processing. Hence, in light of the previous electrophysiological (Hill et al., 1999), neuropsychological (Corral et al., 2003) and neuroimaging (Spadoni et al., 2013) studies in HR offsprings that report developmental delays, our findings could further explain the basis of heightened developmental vulnerability in these individuals, indicating that the protracted neuromaturation of functional networks could underlie externalizing temperaments and disorders, and be a potential mechanism for early-onset drug and alcohol problems.

Furthermore, our results also indicated that the density of FL for alcoholism was associated with progressive reduction in functional network segregation measures. This is consistent with previous studies examining alcoholism family history density (Cservenka et al., 2014, 2015b), suggesting that the HR offspring carry the burden of familial susceptibility, genetic or otherwise, as functional network abnormalities proportional to the degree of their familial loading.

4.4. Lateralization of the small-world deficits

The deficits in functional segregation measures, at brain region that are involved in cognitive control and attention processing, were

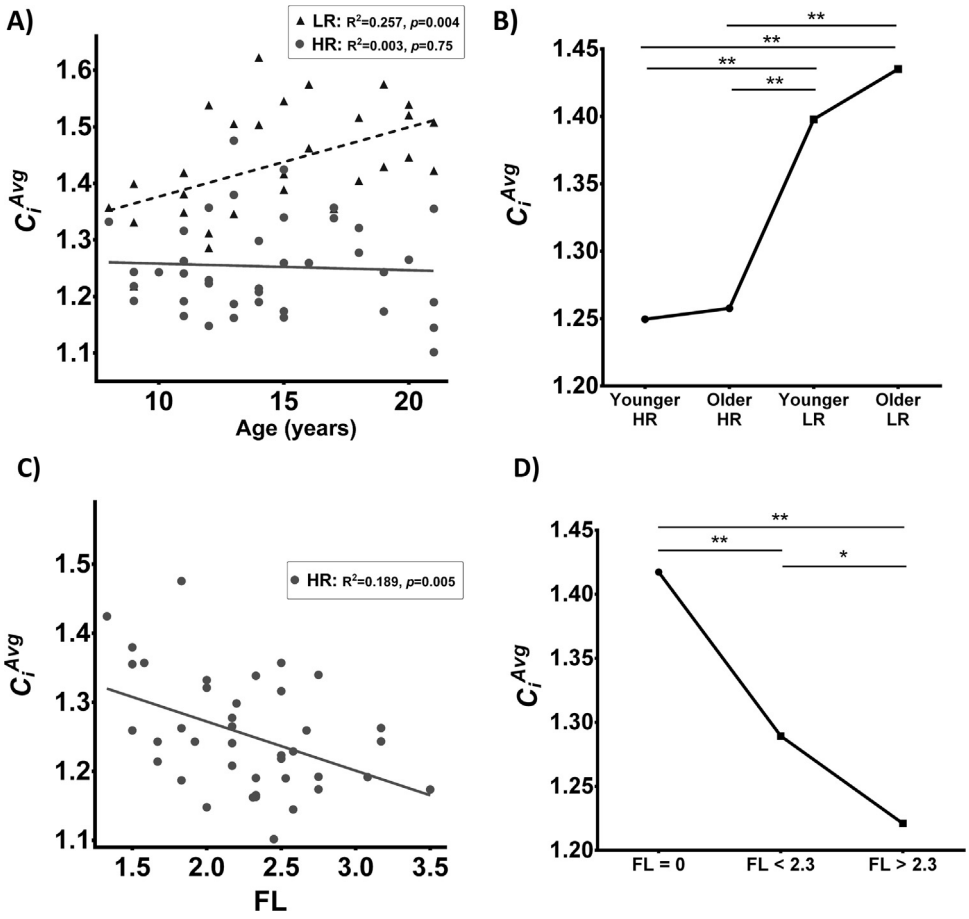

Fig. 4. (A) Regression slopes of the average clustering coefficient value (C_i^{Avg}) of the significant nodes for high-risk (HR) and low-risk (LR) groups over the age range studied, (B) Comparison of C_i^{Avg}across age groups, (C) Regression slopes of C_i^{Avg} for HR group with Family Loading (FL) scores, and (D) Comparison of C_i^{Avg}across AUD FL groups. The symbols (** < 0.001, * < 0.05) indicates significant difference in post-hoc Tukey Test. The functional segregation in HR subjects showed a relatively flat progression from childhood to young adulthood, and was proportional to family loading of AUDs.

lateralized to the right cerebral and contra-lateral cerebellar hemispheres. Given the dominance of right hemisphere for inhibitory control in healthy individuals (Aron et al., 2004; Chikazoe et al., 2007; Garavan et al., 1999) and the fact that right lateralization of abnormalities is a fairly consistent finding in ADHD with resting state (Sripada et al., 2014) and task-related (Depue et al., 2010; Smith et al., 2008) fMRI studies, the lateralization of deficits in our HR sample is significant. Further, an independent large sample of HR offspring with high impulsivity also demonstrated disruptions in orbitofrontal cortex (OFC) laterality with reduced right OFC volume (Hill et al., 2009). Hence, the right lateralized deficits in HR offspring (with externalizing diatheses) could reflect subtle precursors of the bilateral deficits that are seen in adults with AUDs (Beck et al., 2012).

4.5. Disruption in small world architecture – a quantitative endophenotype in the risk to develop alcoholism?

The small-world measures of the resting state functional networks have strong genetic underpinnings and are substantially heritable. (Fornito et al., 2011; Glahn et al., 2010; Smit et al., 2008). Additionally, they also exhibit high phenotypic and genetic stability over developmental age span (Smit et al., 2010). Although the evidence is preliminary, the small world disruptions that were closely linked to the expressed externalizing behaviors and AUD FL density, may be considered as a resting brain network correlate for vulnerability to alcoholism. Future studies should attempt at further characterizing and validating this as a potential endophenotypic marker. Moreover, such individualized risk predictors are vital for any prevention and intervention strategies in at-risk vulnerable population (Hill and O'Brien, 2015).

4.6. Limitations

While this is the first study to examine the small-world architecture of the resting brain in high-risk offspring using graph-theoretical approach, it has certain limitations that should be considered when interpreting the results. First, since this study was a cross-sectional design, it is unclear if the developmental differences that were found across the age groups are indicative of a developmental delay or more severe deficits. Longitudinal investigations in subjects carefully matched for puberty, age and gender will be crucial to understand how the age mediates the functional network maturation in HR offspring. Second, as the rsfMRI based assessments, including those based on graph theoretical analysis, are highly sensitive to head motion we employed a strict threshold for excessive head movements that lead to exclusion of 20 subjects (10 HR and 10 LR). Third, we examined only male offspring of treatment-seeking AUD father. Although, this sampling strategy ensured high density of AUDs in the targeted families, this might limit the generalizability across the gender and non-treatment seeking community families. Fourth, although we explored the relationship of externalizing symptoms with graph-theoretical measures, further examination of its relationship with neuro-cognitive tests are warranted. Finally, although several converging lines of evidence indicate that the functional brain networks in humans do have a small world architecture (Achard and Bullmore, 2007; Bullmore and Sporns, 2009; Salvador et al., 2005), it is still possible that at a structural

cellular level the brain might exhibit large-world properties (Hilgetag and Goulas, 2016). In the current study, technical factors that could artefactually affect the propensity for small-worldness (Hilgetag and Goulas, 2016), were controlled by adopting a spatially coarse-grained parcellation scheme using Dosenbach's functional atlas which uses representative ROI spheres of uniform size. Also, while deriving the binarized connectivity matrices, only the top S% of the strong links over sparsity range were used instead of a single threshold, thus reducing the erroneous influence of weak connections.

4.7. Summary

Externalizing behaviors and temperaments, which increase vulnerability to AUDs, appear to be modulated by developmentally relevant disruptions in small-world architecture of the resting brain in HR offspring. Specifically, several brain regions sub-serving cognitive, affective, and sensorimotor processes, demonstrated significantly reduced functional segregation indicating reduced ability to segregate and specialize information flow efficiently in these regions, which may ultimately contribute to their addiction vulnerability. Our findings add to the nascent literature regarding the role of characterizing resting brain network alterations underlying familial vulnerability to alcoholism in at-risk population. Detection and estimation of these alterations could be vital in understanding the pathobiology of externalizing behaviors as well as familial risk for early-onset alcoholism.

Authors contribution

VB, RDB and GVS were responsible for the study concept and design. VB, RDB, GVS and BH, oversaw data collection. RDB and BB oversaw data analysis. BH and RP conducted the data analysis. VB, RDB, GVS, BB and BH assisted with interpretation of findings. BH drafted the manuscript. VB, RDB, GVS, BB and RP provided critical revision of the manuscript for important intellectual content. All authors critically reviewed content and approved final version for publication.

Conflict of interest

None of the authors have any financial disclosure to make or have any conflict of interest.

Acknowledgments

This study was supported by the Centre for Addiction Medicine, Department of Psychiatry, NIMHANS. The Wellcome Trust/DBT India Alliance supported authors BH (14/1/10012) and GVS (500236/Z/11/Z).

Appendix A. Supporting information

Supplementary data associated with this article can be found in the online version at http://dx.doi.org/10.1016/j.pscychresns.2017.05.002.

References

Achard, S., Bullmore, E., 2007. Efficiency and cost of economical brain functional networks. PLoS Comput. Biol. 3, e17.
Acheson, A., Robinson, J.L., Glahn, D.C., Lovallo, W.R., Fox, P.T., 2009. Differential activation of the anterior cingulate cortex and caudate nucleus during a gambling simulation in persons with a family history of alcoholism: studies from the Oklahoma Family Health Patterns Project. Drug Alcohol Depend. 100, 17–23.
Annett, M., 1967. The binomial distribution of right, mixed and left handedness. Q. J. Exp. Psychol. 19, 327–333.
Aron, A.R., Robbins, T.W., Poldrack, R.A., 2004. Inhibition and the right inferior frontal cortex. Trends Cogn. Sci. 8, 170–177.
Bechara, A., Dolan, S., Hindes, A., 2002. Decision-making and addiction (part II): myopia for the future or hypersensitivity to reward? Neuropsychologia 40, 1690–1705.
Beck, A., Wustenberg, T., Genauck, A., Wrase, J., Schlagenhauf, F., Smolka, M.N., Mann, K., Heinz, A., 2012. Effect of brain structure, brain function, and brain connectivity on relapse in alcohol-dependent patients. Arch. General. Psychiatry 69, 842–852.
Benegal, V., Jain, S., Subbukrishna, D.K., Channabasavanna, S.M., 1995. P300 amplitudes vary inversely with continuum of risk in first degree male relatives of alcoholics. Psychiatr. Genet. 5, 149–156.
Benegal, V., Antony, G., Venkatasubramanian, G., Jayakumar, P.N., 2007. Gray matter volume abnormalities and externalizing symptoms in subjects at high risk for alcohol dependence. Addict. Biol. 12, 122–132.
Biswal, B., Yetkin, F.Z., Haughton, V.M., Hyde, J.S., 1995. Functional connectivity in the motor cortex of resting human brain using echo-planar MRI. Magn. Reson. Med. 34, 537–541.
Bornovalova, M.A., Hicks, B.M., Iacono, W.G., McGue, M., 2010. Familial transmission and heritability of childhood disruptive disorders. Am. J. Psychiatry 167, 1066–1074.
Brook, D.W., Brook, J.S., Zhang, C., Koppel, J., 2010. Association between attention-deficit/hyperactivity disorder in adolescence and substance use disorders in adulthood. Arch. Pediatr. Adolesc. Med. 164, 930–934.
Bucholz, K.K., Cadoret, R., Cloninger, C.R., Dinwiddie, S.H., Hesselbrock, V.M., Nurnberger Jr., J.I., Reich, T., Schmidt, I., Schuckit, M.A., 1994. A new, semi-structured psychiatric interview for use in genetic linkage studies: a report on the reliability of the SSAGA. J. Stud. Alcohol 55, 149–158.
Bullmore, E., Sporns, O., 2009. Complex brain networks: graph theoretical analysis of structural and functional systems. Nat. Rev. Neurosci. 10, 186–198.
Chen, Z., Liu, M., Gross, D.W., Beaulieu, C., 2013. Graph theoretical analysis of developmental patterns of the white matter network. Front. Hum. Neurosci. 7, 716.
Chikazoe, J., Konishi, S., Asari, T., Jimura, K., Miyashita, Y., 2007. Activation of right inferior frontal gyrus during response inhibition across response modalities. J. Cogn. Neurosci. 19, 69–80.
Cloninger, C.R., Sigvardsson, S., Reich, T., Bohman, M., 1986. Inheritance of risk to develop alcoholism. NIDA Res. Monogr. 66, 86–96.
Corral, M., Holguin, S.R., Cadaveira, F., 2003. Neuropsychological characteristics of young children from high-density alcoholism families: a three-year follow-up. J. Stud. Alcohol 64, 195–199.
Cortese, S., Kelly, C., Chabernaud, C., Proal, E., Di Martino, A., Milham, M.P., Castellanos, F.X., 2012. Toward systems neuroscience of ADHD: a meta-analysis of 55 fMRI studies. Am. J. Psychiatry 169, 1038–1055.
Cotton, N.S., 1979. The familial incidence of alcoholism: a review. J. Stud. Alcohol 40, 89–116.
Cservenka, A., 2016. Neurobiological phenotypes associated with a family history of alcoholism. Drug Alcohol Depend. 158, 8–21.
Cservenka, A., Casimo, K., Fair, D.A., Nagel, B.J., 2014. Resting state functional connectivity of the nucleus accumbens in youth with a family history of alcoholism. Psychiatry Res. 221, 210–219.
Cservenka, A., Alarcon, G., Jones, S.A., Nagel, B.J., 2015a. Advances in human neuroconnectivity research: applications for understanding familial history risk for alcoholism. Alcohol Res.: Curr. Rev. 37, 89–95.
Cservenka, A., Gillespie, A.J., Michael, P.G., Nagel, B.J., 2015b. Family history density of alcoholism relates to left nucleus accumbens volume in adolescent girls. J. Stud. Alcohol Drugs 76, 47–56.
Depue, B.E., Burgess, G.C., Willcutt, E.G., Ruzic, L., Banich, M.T., 2010. Inhibitory control of memory retrieval and motor processing associated with the right lateral prefrontal cortex: evidence from deficits in individuals with ADHD. Neuropsychologia 48, 3909–3917.
Dick, D.M., Aliev, F., Wang, J.C., Grucza, R.A., Schuckit, M., Kuperman, S., Kramer, J., Hinrichs, A., Bertelsen, S., Budde, J.P., Hesselbrock, V., Porjesz, B., Edenberg, H.J., Bierut, L.J., Goate, A., 2008. Using dimensional models of externalizing psychopathology to aid in gene identification. Arch. General. Psychiatry 65, 310–318.
Dosenbach, N.U., Fair, D.A., Cohen, A.L., Schlaggar, B.L., Petersen, S.E., 2008. A dual-networks architecture of top-down control. Trends Cogn. Sci. 12, 99–105.
Dosenbach, N.U., Visscher, K.M., Palmer, E.D., Miezin, F.M., Wenger, K.K., Kang, H.C., Burgund, E.D., Grimes, A.L., Schlaggar, B.L., Petersen, S.E., 2006. A core system for the implementation of task sets. Neuron 50, 799–812.
Dosenbach, N.U., Fair, D.A., Miezin, F.M., Cohen, A.L., Wenger, K.K., Dosenbach, R.A., Fox, M.D., Snyder, A.Z., Vincent, J.L., Raichle, M.E., Schlaggar, B.L., Petersen, S.E., 2007. Distinct brain networks for adaptive and stable task control in humans. Proc. Natl. Acad. Sci. USA 104, 11073–11078.
Dosenbach, N.U., Nardos, B., Cohen, A.L., Fair, D.A., Power, J.D., Church, J.A., Nelson, S.M., Wig, G.S., Vogel, A.C., Lessov-Schlaggar, C.N., Barnes, K.A., Dubis, J.W., Feczko, E., Coalson, R.S., Pruett Jr., J.R., Barch, D.M., Petersen, S.E., Schlaggar, B.L., 2010. Prediction of individual brain maturity using fMRI. Science 329, 1358–1361.
Fair, D.A., Nigg, J.T., Iyer, S., Bathula, D., Mills, K.L., Dosenbach, N.U., Schlaggar, B.L., Mennes, M., Gutman, D., Bangaru, S., Buitelaar, J.K., Dickstein, D.P., Di Martino, A., Kennedy, D.N., Kelly, C., Luna, B., Schweitzer, J.B., Velanova, K., Wang, Y.F., Mostofsky, S., Castellanos, F.X., Milham, M.P., 2012. Distinct neural signatures detected for ADHD subtypes after controlling for micro-movements in resting state functional connectivity MRI data. Front. Syst. Neurosci. 6, 80.
Fornito, A., Zalesky, A., Bullmore, E.T., 2010. Network scaling effects in graph analytic studies of human resting-state FMRI data. Front. Syst. Neurosci. 4, 22.
Fornito, A., Zalesky, A., Bassett, D.S., Meunier, D., Ellison-Wright, I., Yucel, M., Wood, S.J., Shaw, K., O'Connor, J., Nertney, D., Mowry, B.J., Pantelis, C., Bullmore, E.T., 2011. Genetic influences on cost-efficient organization of human cortical functional networks. J. Neurosci.: Off. J. Soc. Neurosci. 31, 3261–3270.
Fox, M.D., Raichle, M.E., 2007. Spontaneous fluctuations in brain activity observed with functional magnetic resonance imaging. Nat. Rev. Neurosci. 8, 700–711.

Friston, K.J., Williams, S., Howard, R., Frackowiak, R.S., Turner, R., 1996. Movement-related effects in fMRI time-series. Magn. Reson. Med. 35, 346–355.
Garavan, H., Ross, T.J., Stein, E.A., 1999. Right hemispheric dominance of inhibitory control: an event-related functional MRI study. Proc. Natl. Acad. Sci. USA 96, 8301–8306.
Gierski, F., Hubsch, B., Stefaniak, N., Benzerouk, F., Cuervo-Lombard, C., Bera-Potelle, C., Cohen, R., Kahn, J.P., Limosin, F., 2013. Executive functions in adult offspring of alcohol-dependent probands: toward a cognitive endophenotype? Alcohol., Clin. Exp. Res. 37 (Suppl 1), E356–E363.
Glahn, D.C., Winkler, A.M., Kochunov, P., Almasy, L., Duggirala, R., Carless, M.A., Curran, J.C., Olvera, R.L., Laird, A.R., Smith, S.M., Beckmann, C.F., Fox, P.T., Blangero, J., 2010. Genetic control over the resting brain. Proc. Natl. Acad. Sci. USA 107, 1223–1228.
Goodwin, D.W., 1979. Alcoholism and heredity. A review and hypothesis. Arch. Gen. Psychiatry 36, 57–61.
Hauser, T.U., Iannaccone, R., Ball, J., Mathys, C., Brandeis, D., Walitza, S., Brem, S., 2014. Role of the medial prefrontal cortex in impaired decision making in juvenile attention-deficit/hyperactivity disorder. JAMA Psychiatry 71, 1165–1173.
He, Y., Dagher, A., Chen, Z., Charil, A., Zijdenbos, A., Worsley, K., Evans, A., 2009. Impaired small-world efficiency in structural cortical networks in multiple sclerosis associated with white matter lesion load. Brain: J. Neurol. 132, 3366–3379.
Herting, M.M., Fair, D., Nagel, B.J., 2011. Altered fronto-cerebellar connectivity in alcohol-naive youth with a family history of alcoholism. NeuroImage 54, 2582–2589.
Hicks, B.M., Foster, K.T., Iacono, W.G., McGue, M., 2013. Genetic and environmental influences on the familial transmission of externalizing disorders in adoptive and twin offspring. JAMA Psychiatry 70, 1076–1083.
Hilgetag, C.C., Goulas, A., 2016. Is the brain really a small-world network? Brain Struct. Funct. 221, 2361–2366.
Hill, S.Y., O'Brien, J., 2015. Psychological and neurobiological precursors of alcohol use disorders in high risk youth. Curr. Addict. Rep. 2, 104–113.
Hill, S.Y., Wang, S., Carter, H., McDermott, M.D., Zezza, N., Stiffler, S., 2013. Amygdala volume in offspring from multiplex for alcohol dependence families: the moderating influence of childhood environment and 5-HTTLPR variation. J. Alcohol. Drug Depend.(Suppl. 1).
Hill, S.Y., Shen, S., Locke, J., Steinhauer, S.R., Konicky, C., Lowers, L., Connolly, J., 1999. Developmental delay in P300 production in children at high risk for developing alcohol-related disorders. Biol. Psychiatry 46, 970–981.
Hill, S.Y., Wang, S., Carter, H., Tessner, K., Holmes, B., McDermott, M., Zezza, N., Stiffler, S., 2011. Cerebellum volume in high-risk offspring from multiplex alcohol dependence families: association with allelic variation in GABRA2 and BDNF. Psychiatry Res. 194, 304–313.
Hill, S.Y., Wang, S., Kostelnik, B., Carter, H., Holmes, B., McDermott, M., Zezza, N., Stiffler, S., Keshavan, M.S., 2009. Disruption of orbitofrontal cortex laterality in offspring from multiplex alcohol dependence families. Biol. Psychiatry 65, 129–136.
Hussong, A., Bauer, D., Chassin, L., 2008. Telescoped trajectories from alcohol initiation to disorder in children of alcoholic parents. J. Abnorm. Psychol. 117, 63–78.
Hussong, A.M., Wirth, R.J., Edwards, M.C., Curran, P.J., Chassin, L.A., Zucker, R.A., 2007. Externalizing symptoms among children of alcoholic parents: entry points for an antisocial pathway to alcoholism. J. Abnorm. Psychol. 116, 529–542.
Jacob, T., Waterman, B., Heath, A., True, W., Bucholz, K.K., Haber, R., Scherrer, J., Fu, Q., 2003. Genetic and environmental effects on offspring alcoholism: new insights using an offspring-of-twins design. Arch. Gen. Psychiatry 60, 1265–1272.
Krueger, R.F., Markon, K.E., Patrick, C.J., Iacono, W.G., 2005. Externalizing psychopathology in adulthood: a dimensional-spectrum conceptualization and its implications for DSM-V. J. Abnorm. Psychol. 114, 537–550.
Kumar, N., Gupta, N., Kishore, J., 2012. Kuppuswamy's socioeconomic scale: updating income ranges for the year 2012. Indian J. Public Health 56, 103–104.
Kuperman, S., Chan, G., Kramer, J.R., Bierut, L., Bucholz, K.K., Fox, L., Hesselbrock, V., Numberger Jr., J.I., Reich, T., Reich, W., Schuckit, M.A., Collaborative Study on the Genetics of, A, 2005. Relationship of age of first drink to child behavioral problems and family psychopathology. Alcohol. Clin. Exp. Res. 29, 1869–1876.
Lee, M.H., Smyser, C.D., Shimony, J.S., 2013. Resting-state fMRI: a review of methods and clinical applications. AJNR Am. J. Neuroradiol. 34, 1866–1872.
Lewis, S.W., Murray, R.M., 1987. Obstetric complications, neurodevelopmental deviance, and risk of schizophrenia. J. Psychiatr. Res. 21, 413–421.
MacDonald 3rd, A.W., Cohen, J.D., Stenger, V.A., Carter, C.S., 2000. Dissociating the role of the dorsolateral prefrontal and anterior cingulate cortex in cognitive control. Science 288, 1835–1838.
Maxwell, M., 1992. Family Interview for Genetic Studies (FIGS): A Manual for FIGS, Clinical Neurogenetics Branch, Intramural Research Program. National Institute of Mental Health, Bethesda, MD.
McGue, M., Iacono, W.G., Legrand, L.N., Malone, S., Elkins, I., 2001. Origins and consequences of age at first drink. I. Associations with substance-use disorders, disinhibitory behavior and psychopathology, and P3 amplitude. Alcohol. Clin. Exp. Res. 25, 1156–1165.
Nigg, J.T., Glass, J.M., Wong, M.M., Poon, E., Jester, J.M., Fitzgerald, H.E., Puttler, L.I., Adams, K.M., Zucker, R.A., 2004. Neuropsychological executive functioning in children at elevated risk for alcoholism: findings in early adolescence. J. Abnorm. Psychol. 113, 302–314.
Power, J.D., Schlaggar, B.L., Petersen, S.E., 2015. Recent progress and outstanding issues in motion correction in resting state fMRI. NeuroImage 105, 536–551.
Power, J.D., Barnes, K.A., Snyder, A.Z., Schlaggar, B.L., Petersen, S.E., 2012. Spurious but systematic correlations in functional connectivity MRI networks arise from subject motion. NeuroImage 59, 2142–2154.
Rangaswamy, M., Porjesz, B., Ardekani, B.A., Choi, S.J., Tanabe, J.L., Lim, K.O., Begleiter, H., 2004. A functional MRI study of visual oddball: evidence for frontoparietal dysfunction in subjects at risk for alcoholism. Neuroimage 21, 329–339.
Rubinov, M., Sporns, O., 2010. Complex network measures of brain connectivity: uses and interpretations. NeuroImage 52, 1059–1069.
Salvador, R., Suckling, J., Coleman, M.R., Pickard, J.D., Menon, D., Bullmore, E., 2005. Neurophysiological architecture of functional magnetic resonance images of human brain. Cereb. cortex 15, 1332–1342.
Salvatore, J.E., Gottesman, I.I., Dick, D.M., 2015. Endophenotypes for alcohol use disorder: an update on the field. Curr. Addict. Rep. 2, 76–90.
Sato, J.R., Salum, G.A., Gadelha, A., Picon, F.A., Pan, P.M., Vieira, G., Zugman, A., Hoexter, M.Q., Anes, M., Moura, L.M., Gomes Del'Aquilla, M.A., Amaro Jr., E., McGuire, P., Crossley, N., Lacerda, A., Rohde, L.A., Miguel, E.C., Bressan, R.A., Jackowski, A.P., 2014. Age effects on the default mode and control networks in typically developing children. J. Psychiatr. Res. 58, 89–95.
Schuckit, M.A., 1985. Genetics and the risk for alcoholism. JAMA 254, 2614–2617.
Schweinsburg, A.D., Paulus, M.P., Barlett, V.C., Killeen, L.A., Caldwell, L.C., Pulido, C., Brown, S.A., Tapert, S.F., 2004. An FMRI study of response inhibition in youths with a family history of alcoholism. Ann. N.Y. Acad. Sci. 1021, 391–394.
Silveri, M.M., Rogowska, J., McCaffrey, A., Yurgelun-Todd, D.A., 2011. Adolescents at risk for alcohol abuse demonstrate altered frontal lobe activation during Stroop performance. Alcohol.: Clin. Exp. Res. 35, 218–228.
Smit, D.J., Stam, C.J., Posthuma, D., Boomsma, D.I., de Geus, E.J., 2008. Heritability of "small-world" networks in the brain: a graph theoretical analysis of resting-state EEG functional connectivity. Hum. Brain Mapp. 29, 1368–1378.
Smit, D.J., Boersma, M., van Beijsterveldt, C.E., Posthuma, D., Boomsma, D.I., Stam, C.J., de Geus, E.J., 2010. Endophenotypes in a dynamically connected brain. Behav. Genet. 40, 167–177.
Smith, A.B., Taylor, E., Brammer, M., Halari, R., Rubia, K., 2008. Reduced activation in right lateral prefrontal cortex and anterior cingulate gyrus in medication-naive adolescents with attention deficit hyperactivity disorder during time discrimination. J. Child Psychol. Psychiatry Allied Discip. 49, 977–985.
Snedecor, G.W., Cochran, W.G., 1989. Statistical Methods, 8th ed. Iowa State Univ. Press Iowa, Ames.
Spadoni, A.D., Simmons, A.N., Yang, T.T., Tapert, S.F., 2013. Family history of alcohol use disorders and neuromaturation: a functional connectivity study with adolescents. Am. J. Drug Alcohol Abus. 39, 356–364.
Sporns, O., Chialvo, D.R., Kaiser, M., Hilgetag, C.C., 2004. Organization, development and function of complex brain networks. Trends Cogn. Sci. 8, 418–425.
Sripada, C., Kessler, D., Fang, Y., Welsh, R.C., Prem Kumar, K., Angstadt, M., 2014. Disrupted network architecture of the resting brain in attention-deficit/hyperactivity disorder. Hum. Brain Mapp. 35, 4693–4705.
Turner, W.M., Cutter, H.S., Worobec, T.G., O'Farrell, T.J., Bayog, R.D., Tsuang, M.T., 1993. Family history models of alcoholism: age of onset, consequences and dependence. J. Stud. Alcohol 54, 164–171.
Venkatasubramanian, G., Anthony, G., Reddy, U.S., Reddy, V.V., Jayakumar, P.N., Benegal, V., 2007. Corpus callosum abnormalities associated with greater externalizing behaviors in subjects at high risk for alcohol dependence. Psychiatry Res. 156, 209–215.
Verhulst, B., Neale, M.C., Kendler, K.S., 2015. The heritability of alcohol use disorders: a meta-analysis of twin and adoption studies. Psychol. Med. 45, 1061–1072.
Vogel, A.C., Church, J.A., Power, J.D., Miezin, F.M., Petersen, S.E., Schlaggar, B.L., 2013. Functional network architecture of reading-related regions across development. Brain Lang. 125, 231–243.
Watts, D.J., Strogatz, S.H., 1998. Collective dynamics of 'small-world' networks. Nature 393, 440–442.
Wetherill, R.R., Bava, S., Thompson, W.K., Boucquey, V., Pulido, C., Yang, T.T., Tapert, S.F., 2012. Frontoparietal connectivity in substance-naive youth with and without a family history of alcoholism. Brain Res. 1432, 66–73.
Witkiewitz, K., King, K., McMahon, R.J., Wu, J., Luk, J., Bierman, K.L., Coie, J.D., Dodge, K.A., Greenberg, M.T., Lochman, J.E., Pinderhughes, E.E., Conduct Problems Prevention Research, G, 2013. Evidence for a multi-dimensional latent structural model of externalizing disorders. J. Abnorm. Child Psychol. 41, 223–237.